

Overlapping Difference Expansion Reversible Data Hiding

Chin-Feng Lee¹, Jau-Ji Shen², and Chin-Yung Wu²

(Corresponding author: Chin-Feng Lee)

Department of Information Management, Chaoyang University of Technology¹

Taichung 41349, Taiwan, ROC

Email: lcf@cyut.edu.tw

TManagement Information Systems, National Chung Hsing University²

Taichung, Taiwan, ROC

(Received Aug. 15, 2022; Revised and Accepted Jan. 28, 2023; First Online Feb. 17, 2023)

The Special Issue on Trusted ICT Technologies on the Smart Society and Secure Multimedia Applications

Special Editor: Prof. Chin-Feng Lee (Chaoyang University of Technology)

Abstract

Rapid technological development has made information transmission convenient by using the internet in the shortest possible time. Despite this, there is an increase in information security problems. Therefore, the need for information hiding is of paramount importance to the public. The difference expansion (DE) embedding technology has good embedding capacity in reversible data hiding (RDH) technology. However, the DE embedding technique creates problems in the multi-layer embedding process. This study proposes an embedding strategy of horizontal overlapping and vertical overlapping difference expansion (also called HoVo_DE for short) to enhance the information embedding of the DE series methods and improve the problem of difference expansion cascading caused by multiple DE embedding. The experimental results show that the proposed strategy reduces the distortion of image quality and has a higher embedding capacity than other strategies.

Keywords: Data Hiding; Reversible Data Hiding; Difference Expansion (DE); Improved Reduced Difference Expansion (IRDE)

1 Introduction

The emergence of communication software and social platforms has significantly enhanced communication and information sharing in the shortest possible time. One of the most integral parts of network operation and maintenance is network security. A large number of multimedia forensics and network security technologies have aroused extensive research attention in multimedia data integrity assessment [11]. Also, there is a rapid increase in information security problems. Thus, transmitting messages

safely and freely on the internet has become a concern. Information hiding [3] involves embedding secret data in digital multimedia carriers, such as images or documents. In the case of digital images, the difference between the cover image before embedding the secret message and the stego-image after embedding should be as far as possible to ensure the secrecy and security of the embedded secret information [1, 4]. This way, the slight difference between the mask and the camouflage image can effectively prevent encrypted information from being detected or deciphered during the transmission process. Information hiding can be classified as irreversible data hiding [6] and reversible data hiding (RDH) [2, 5, 7–10, 12–17].

Among several RDH methods, the difference expansion (DE) method proposed by Tian in 2003 [17], the prediction error expansion (PEE) method proposed by Thodi *et al.* in 2004 [12], histogram shifting (HS) method proposed by Ni *et al.* in 2006 [7], and pixel value ordering (PVO) method proposed by Li *et al.* in 2013 [8]. Among these methods, the highly efficient and well-known is the DE method, which can achieve the effect of high embedding quantity through a relatively simple and low-complexity operation process. The DE method uses the difference between the adjacent pixel pair and the average value to embed the secret data at the adjacent pixel pair such that the average value at the adjacent pixel pair remains unchanged.

The intuitive and concise methods for embedding secret data through the difference expansion between pixel pair have significantly attracted much interest to optimize the DE and derive several DE series methods with better performance [5, 14, 15]. Liu *et al.* [2] proposed the reduced DE (RDE) strategy in 2007 to solve the image distortion problem of the DE scheme. After the secret information is embedded, the RDE strategy can reduce the original difference between the two stego-pixels to enable the re-

duction of the degree of distortion. Then, Yi et al. [9] proposed the improved reduced difference expansion (also referred as IRDE) method in 2009. The IRDE method uses a logarithmic transformation function to reduce the difference first before the secret information has been embedded so that the difference between stego-pixels can be minimized more effectively, thereby maintaining good image quality. Alattar [10] proposed the Quad-DE method which introduces the difference expansion hiding within a group of pixels on the basis of 2×2 blocks. Lee *et al.* proposed block-shiftable embedding (BSE) method [13] based on the DE scheme. The method of block displacement increases the embedded embedding capacity while retaining the image quality within an acceptable range.

The DE embedding technology has a good embedding capacity; however, there is an inherent weakness in the DE embedding scheme, i.e., it will cause the cascading problem due to continuous differential expansion in the multi-layer embedding process. Each embedding represents an expansion of the difference value, so after the difference value of the multi-layer embedded image is expanded to a degree, the relative image quality dramatically decreases. Therefore, this study proposes an embedding strategy of horizontal overlapping and vertical overlapping DE, also called HoVo_DE for short to simultaneously enhance the embedding capacity and improve the problem of DE cascading caused by multiple-layer embedding. Exploring the relationship between different block sizes and making full use of the image quality in the blocks, the proposed embedding strategy of HoVo_DE can effectively suppress the occurrence of the DE cascading problem.

2 Block-Shiftable Embedding

Lee *et al.* proposed the block-shiftable embedding (also referred as BSE) [13] strategy for reversible data hiding. Because the traditional multi-layer embedding strategy can adversely distort the image quality, the BSE strategy shifts the block and changes the embedding starting point during the second layer embedding, which can improve the image quality and increase the embedding capacity.

The BSE strategy employs the DE manipulation with different block segmentation for embedding. The first step is to divide the original image I of size $W \times H$ into non-overlapping pixel pairs of size 1×2 individually. The pixel pairs of the first layer and second layer are as shown in Figures 1(a) and 1(b) respectively. Then the BSE performs the DE embedding operation on each pixel pair in the sequence.

In the previous method, the secret data will be embedded in one layer and then start to embed the remaining information into the second layer. However, the BSE strategy spreads the secret data in two layers according to the division mode of different blocks with a proper threshold. By using different partitioning schemes for each embedding layer, the predictions become adaptive, creating

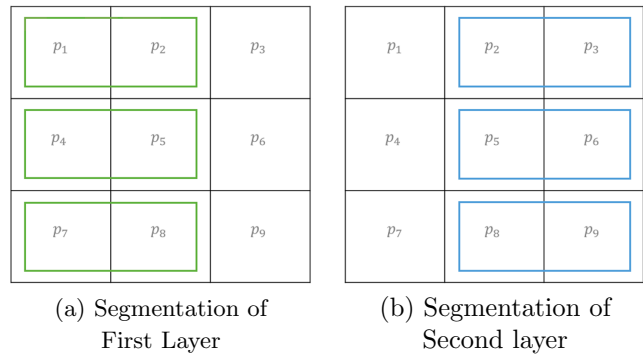


Figure 1: The Block-Shiftable embedding strategy.

more room for improvement over previous state-of-the-art methods. More, secret data will be hidden in smoother blocks and thus have better image quality.

3 Proposed Method

The problem of difference expansion cascading exists in the traditional DE and the IRDE methods, after multiple-layer embedding has been performed to a certain extent. The differential expansion cascade problem will prevent adjacent pixel pairs from being able to hide data or cause serious image distortion. We propose an embedding strategy of horizontal overlapping and vertical overlapping DE strategy, also called HoVo_DE embedding strategy for short, which is different from the previous DE based methods and performs overlapping embedding in the horizontal and vertical directions, respectively. In the experiment, we applied the HoVo_DE embedding strategy under different block segmentation modes and discussed the cover image's embedding capacity and the stego-image's quality.

3.1 HoVo Difference Embedding Strategy

The HoVo difference embedding strategy (also called as the HoVo_DE embedding strategy for short) proposed in this study divides the original image into non-overlapping blocks with $M \times N$ pixels before embedding. Independent embedding is performed in each block. Thus, the differential expansion cascading can be limited to the current block to avoid affecting the pixels of other blocks. The division of blocks can suppress the chain reaction of differential expansion cascading and reduce the degree of image quality damage. Figure 2 shows that, compared with the traditional multi-layer embedding mode, our proposed HoVo_DE embedding strategy, performing information hiding after block division can suppress the rapid expansion of camouflaged pixel values caused by DE cascades to a certain extent.

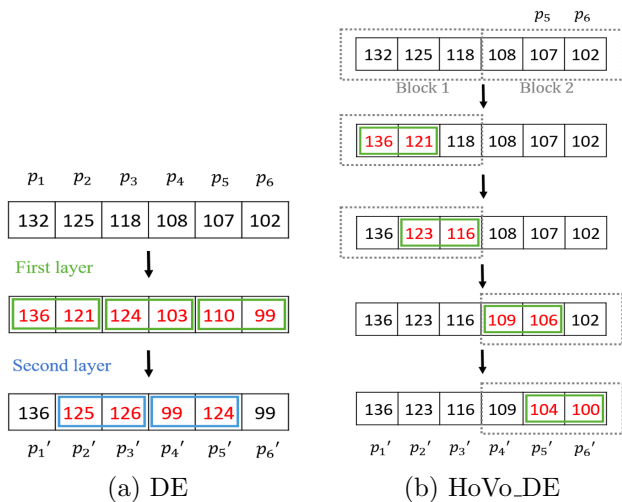


Figure 2: Difference expansion cascading methods. (a) DE method (b) the HoVo_DE embedding method

The proposed HoVo_DE embedding strategy uses four different block division modes, namely, 3×3 , 4×4 , 5×5 , and 6×6 . Figure 3 below shows the group overlapping modes with the block size of 6×6 .

3.2 Embedding Procedure

The embedding steps are as follows.

Algorithm 1 The embedding procedure

- 1: Obtain the cover image I with an image size of $W \times H$.
 - 2: Divide I into non-overlapping blocks of size $M \times N$ in sequence from top to bottom and left to right.
 - 3: Each block is divided into groups. There are $M \times (N - 1)$ groups in the horizontal direction and $N \times (M - 1)$ groups in the vertical direction; that is, a total of $M(N - 1) + N(M - 1)$ groups in a block.
 - 4: According to the HoVo_DE embedding strategy, the information hiding method of DE or IRDE is employed to hide the secret data bits in each group of every row by overlapping groups from both ends of the block to the middle of the block.
 - 5: The DE or IRDE method hides the secret data bits in each group of every column by overlapping groups from both ends of the block to the middle of the block.
-

3.3 Example of HoVo_DE Embedding Strategy

The following example comes from the HoVo_DE embedding strategy applied to the 3×3 block size. There are a total of $3 \times (3 - 1) + 3 \times (3 - 1) = 12$ groups can be used in one block.

Assume that the first group, denoted by $g_1 = (p_1, p_2) = (132, 125)$. Assuming that the to-be hidden secret data bit is 1, after the DE method is applied to the first group, we

can obtain $g_1 = (p'_1, p'_2) = (136, 121)$. Next, the embedding operation of g_2 is performed. Therefore, the pixel values used in the group g_2 are (p'_2, p_3) . Repeat the embedding step in sequence until all groups are embedded. Figure 4 presents the flowchart of HoVo_DE embedding strategy in block size 3×3 .

While taking out the secret information and restoring the original image, the operations are performed on each group individually in reverse order, the order should be $g'_{12}, g'_{11}, g'_{10}, \dots, g'_2$, and g'_1 , respectively.

4 Experimental Results

This experiment was performed using MATLAB R2020a installed on the Intel (R) Core (TM) i7-9750 H CPU 2.60 GH-z, 16 GB RAM environment. To quantify the effectiveness of this experimental method and compare it with other related methods, eight standard grayscale images of size 512×512 are used to test the data hiding performance. The test images are Lena, Airplane, Baboon, Boat, Peppers, and Elaine, which can be seen in Figure 5. Additionally, the secret messages hidden in this experiment were all generated using binary random numbers (0 and 1).

This experiment uses two metrics to evaluate the performance of the experimental results, namely, embedding capacity (EC) and peak signal-to-noise ratio (PSNR). The EC represents the amount of secret information in bits that can be embedded in an image. The higher the value of EC, the more information is embedded. The pixel similarity between the cover image and the stego-image is calculated using the PSNR metric. If the PSNR value is high, the more similar the stego-image will be to the original image.

The following sections explore the embedding methods based on DE [17] and IRDE [9] and use the HoVo_DE embedding strategy to achieve the embedding effect under different block sizes.

4.1 Embedding capacity of HoVo_DE Embedding Strategy

This section presents the results of a series of methods using the proposed HoVo_DE embedding strategy. We used the DE and IRDE methods to conduct embedding experiments under different block sizes and compared the results of the DE [17], IRDE [9], and BSE [13] methods. This study mainly explores whether the HoVo_DE embedding strategy can obtain better embedding capacity and image quality with the block size expansion. Under the experiments of various block sizes, the average performance of the IRDE is better than that of the DE. The detailed experimental data below also confirm this findings.

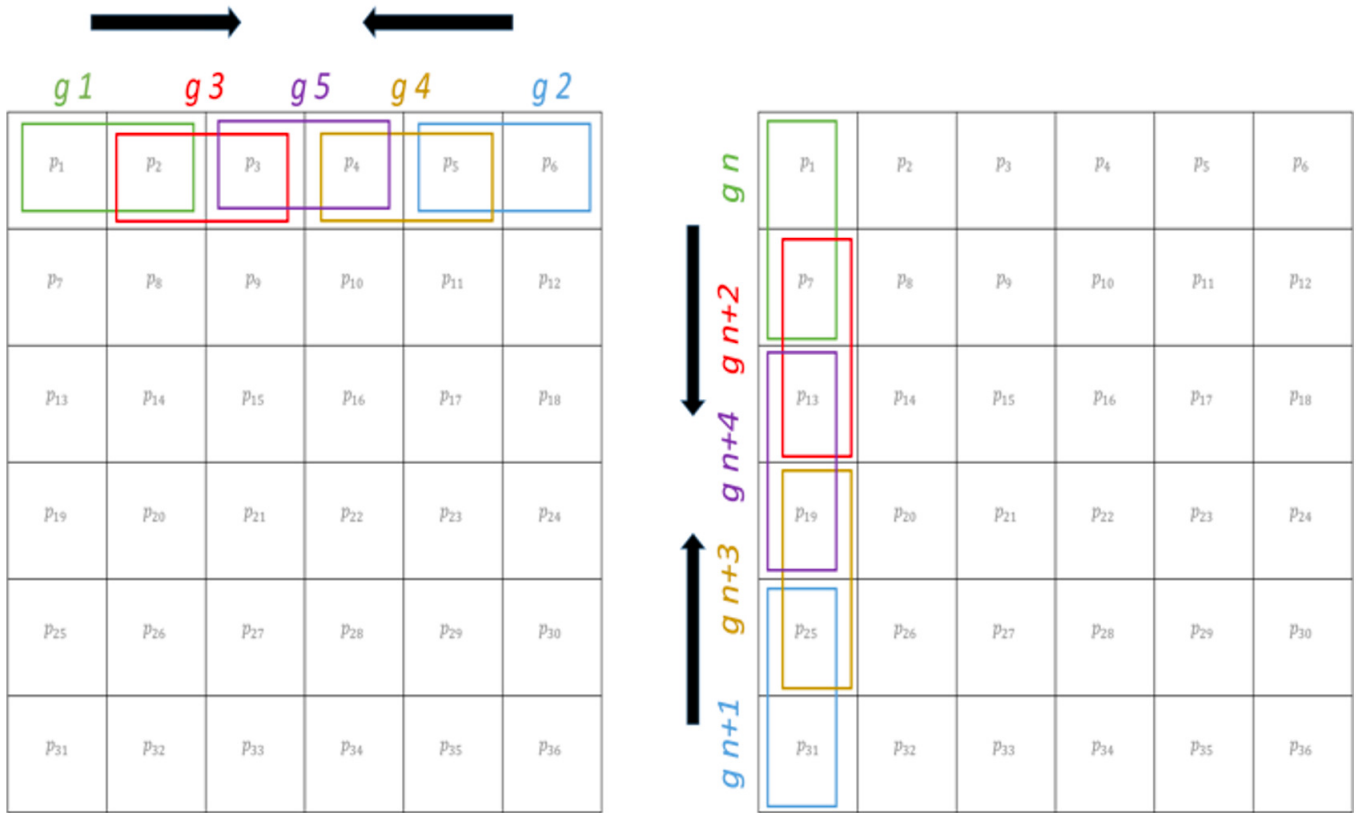


Figure 3: HoVo_DE embedding strategy in block size 6×6

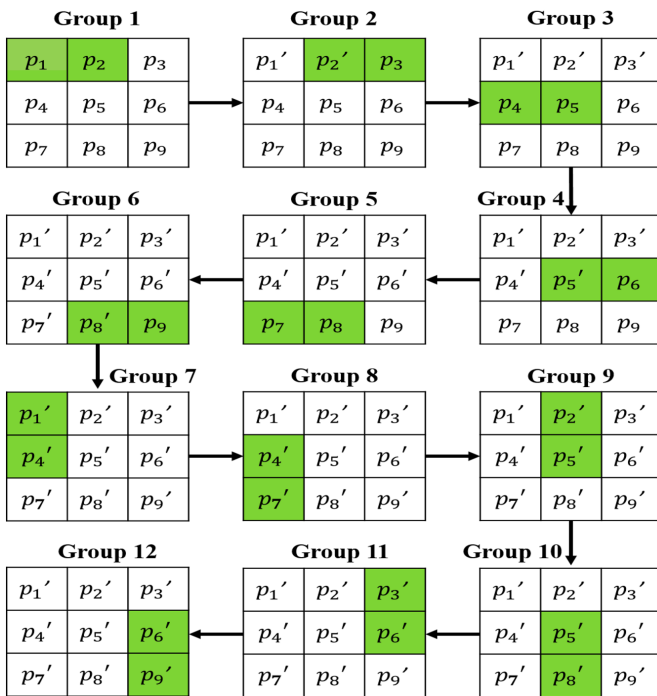


Figure 4: Embedding flowchart of HoV_DE embedding strategy in block size 3×3.

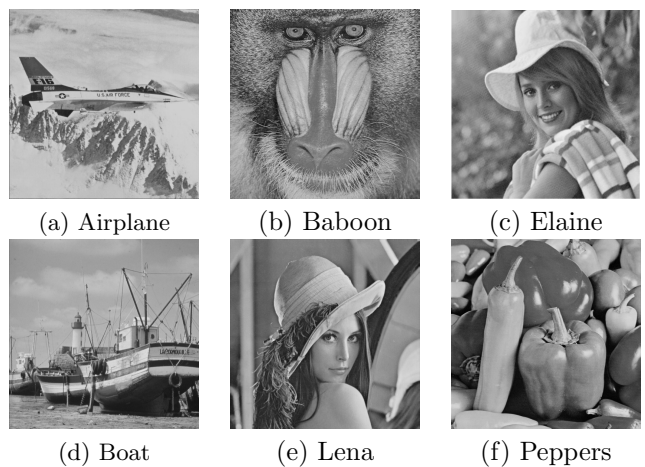


Figure 5: Testing images: (a) Airplane, (b) Baboon, (c) Elaine, (d) Boat, (e) Lena, and (f) Peppers.

4.1.1 HoVo_DE Embedding Strategy Using the DE Method

We implemented the HoVo_DE embedding strategy using the DE and measured the size of different blocks based on the concept of dicing. Furthermore, we determined whether larger blocks can be used to obtain higher embedding capacity while maintaining a certain level of storage image quality. In the following table, DE represents the original DE method; BSE_M×N represents the BSE method implemented in the $M \times N$ block by the DE method; HoVo_DE_M×N represents the use of the HoVo_DE embedding strategy to implement the DE method based on the $M \times N$ block division mode. By implementing HoVo_DE_3×3, HoVo_DE_4×4, HoVo_DE_5×5, and HoVo_DE_6×6, with Lee *et al.*'s BSE_1×4 and BSE_2×2 methods [13], and the original DE method [17]. The table below shows the embedding capacity and image quality for method comparison.

From Table 1, the average embedding capacity of HoVo_DE_3×3, HoVo_DE_4×4, HoVo_DE_5×5, and HoVo_DE_6×6 are 344,951, 390,761, 413,258, 430,226 bits, respectively. We observed that the embedding capacity can be effectively increased when the HoVo_DE embedding strategy is implemented in a larger block division mode. Moreover, compared with our proposed method, the original DE method has only 130,720 bits, and the BSE_2×2 method implemented by DE has 261,675 bits in terms of the average embedding capacity. In this study, the average embedding capacity of the method in the block division modes of HoVo_DE_3×3, HoVo_DE_4×4, HoVo_DE_5×5, and HoVo_DE_6×6 are 2.64 times, 2.99 times, 3.16 times, 3.29 times than that of the DE method, respectively. They are also 1.32, 1.49, 1.58, and 1.65 times than that of the BSE_2×2 method, respectively.

Table 2 shows the stego-image quality measured by PSNR values by the original DE method, BSE_1×4 method, BSE_2×2 method, and our proposed methods with four block division modes which are HoVo_DE_3×3, HoVo_DE_4×4, HoVo_DE_5×5, and HoVo_DE_6×6, respectively.

Table 1: Embedding Capacity of Original DE, BSE and the proposed HoVo DE Embedding Methods

EC	DE	BSE_1×4	BSE_2×2	HoVo_DE_3×3	HoVo_DE_4×4	HoVo_DE_5×5	HoVo_DE_6×6
Airplane	130700	196249	262045	346252	392637	415566	432859
Baboon	130954	196597	261061	341373	386262	408236	424544
Elaine	131060	196560	262012	345374	390707	412548	429477
Boat	130307	196030	261759	345287	391277	413895	430811
Lena	131014	196590	262113	346604	393034	415944	433263
Peppers	130283	196060	261059	344814	390648	413361	430403
Average	130720	196348	261675	344951	390761	413258	430226

When comparing the BSE and HoVo_DE embedding methods for the Airplane, Lena, Peppers images with clear black and white boundaries, in Table 2, the PSNR performance of BSE_1×4 is the best. To the best of our knowledge, this is due to the different block-division structures. As a re-

Table 2: PSNR of Original DE, BSE and the proposed HoVo DE Embedding Methods

PSNR	DE	BSE_1×4	BSE_2×2	HoVo_DE_3×3	HoVo_DE_4×4	HoVo_DE_5×5	HoVo_DE_6×6
Airplane	32.63	31.86	30.58	29.22	26.86	26.79	26.46
Baboon	27.16	28.55	22.53	20.50	19.78	19.53	19.33
Elaine	33.41	30.01	26.57	21.84	20.21	19.51	19.16
Boat	30.59	28.56	27.94	25.54	24.80	24.22	23.95
Lena	33.15	33.54	30.58	29.15	28.59	28.29	27.98
Peppers	33.63	34.69	31.12	29.00	27.92	27.50	27.16
Average	31.76	31.20	27.94	25.62	24.69	24.29	23.98

sult, the BSE_1×4 blocks have a rectangular structure, whereas the blocks of BSE_2×2, HoVo_DE_3×3, HoVo_DE_4×4, HoVo_DE_5×5, and HoVo_DE_6×6 are all square structures. Therefore, BSE_2×2, HoVo_DE_3×3, HoVo_DE_4×4, HoVo_DE_5×5, and HoVo_DE_6×6 have a high probability of overlapping with the black and white boundaries in the images when calculating the pixel differences. The difference at the boundary will be relatively large and the image quality will be degraded. Also, from the above experimental results, the proposed method can successfully obtain a larger embedding capacity than other methods using a larger block size division strategy. With an increase in the block size, the image quality declines but maintains a certain level.

4.1.2 HoVo_DE Embedding Strategy Using the IRDE Method

We implemented the proposed HoVo_DE embedding strategy using the IRDE method [9] and measured the size of different block divisions. Furthermore, we test whether larger blocks can be used to obtain higher embedding capacity while maintaining a certain level of storage image quality. In the following table, IRDE represents the IRDE method; BSE_M×N represents the BSE method implemented in the $M \times N$ block by the IRDE method; HoVo_IRDE_M×N represents the use of the HoVo_DE embedding strategy to implement the IRDE method based on the $M \times N$ block division mode. By implementing HoVo_IRDE_3×3, HoVo_IRDE_4×4, HoVo_IRDE_5×5, and HoVo_IRDE_6×6, with Lee *et al.*'s BSE_1×4 and BSE_2×2 methods [9], and Yi *et al.*'s IRDE methods [9]. The table below shows the embedding capacity and image quality for method comparison.

From Table 3, the average embedding capacity of HoVo_IRDE_3×3, HoVo_IRDE_4×4, HoVo_IRDE_5×5, and HoVo_IRDE_6×6 are 346,786, 393,197, 416,154, 433,496 bits, respectively. We observed that the embedding capacity can be effectively increased when the HoVo_DE embedding strategy is implemented in a larger block division mode. Moreover, compared with our proposed method, the IRDE method has only 131,053 bits, and the BSE_2×2 method implemented by IRDE has 262,111 bits, in terms of the average embedding capacity. In this study, the average embedding capacity of the method in the block division modes of HoVo_IRDE_3×3, HoVo_IRDE_4×4, HoVo_IRDE_5×5,

and HoVo_IRDE_6×6 are 2.65 times, 3.00 times, 3.18 times, 3.30 times that of the IRDE method, respectively. They are also 1.32, 1.50, 1.59, and 1.65 times that of the BSE_2×2 method, respectively. Table 4 shows the stego-image quality measured by PSNR values by the IRDE method, BSE_1×4 method, BSE_2×2 method, and our proposed methods with four block division modes.

Consider the Lena image with BSE_2×2 as an example; Table 3 shows the maximum embedding capacity of 262,145 bits, and Table 4 shows that the PSNR value is 44.28 dB. Table 3 shows that the embedding capacity of HoVo_IRDE_3×3 is increased by 84,656 (=346801-262145) bits compared with that of BSE_2×2. In Table 4, the Lena image using HoVo_IRDE_3×3 shows that its PSNR value is only 1.31 dB lower than that of BSE_2×2. It can be seen in Table 4 that the embedding capacity of the Lena image implemented by HoVo_IRDE_6×6 is increased by 171,356 (=433501-262145) bits compared with the BSE_2×2 method.

Tables 3 and 4 show that the HoVo_DE embedding strategy conducted by IRDE method achieves excellent results in embedding capacity and image quality. Consider the Airplane image as an example, we observe that the embedding capacity of HoVo_IRDE_6×6 in Table 3 is nearly 300% higher than that of the original IRDE, and Table 4 shows that the PSNR of HoVo_IRDE_6×6 can still reach an image quality of about 40 dB without significant degradation. Generally, the higher the embedding capacity, the greater the degree of image distortion. These data show that despite doubling the amount of information embedded, the level of image distortion did not drop in proportion to the sharp drop but decreased slightly to maintain good image quality.

Table 3: Embedding Capacity of IRDE, BSE and the proposed HoVo_IRDE Embedding Methods

EC	IRDE	BSE_1×4	BSE_2×2	HoVo_DE_3×3	HoVo_DE_4×4	HoVo_DE_5×5	HoVo_DE_6×6
Airplane	131072	196608	262144	346804	393217	416154	433473
Baboon	131070	196617	262107	346801	393215	416139	433516
Elaine	131071	196609	262128	346805	393117	416191	433506
Boat	131025	196573	262098	346764	393186	416182	433455
Lena	131072	196609	262145	346801	393207	416161	433501
Peppers	131006	196546	262046	346738	393127	416098	433524
Average	131053	196594	262111	346786	393197	416154	433496

Table 4: PSNR of IRDE, BSE and the proposed HoVo_IRDE Embedding Methods

PSNR	IRDE	BSE_1×4	BSE_2×2	HoVo_DE_3×3	HoVo_DE_4×4	HoVo_DE_5×5	HoVo_DE_6×6
Airplane	45.47	44.36	42.41	41.84	40.98	40.08	38.49
Baboon	42.11	41.70	37.92	36.49	35.91	35.60	34.02
Elaine	46.62	44.55	42.67	40.79	40.22	39.78	38.67
Boat	43.18	42.53	42.00	40.47	39.93	39.59	38.07
Lena	45.83	45.53	44.28	42.97	42.34	42.07	40.84
Peppers	46.70	46.44	44.40	42.90	42.38	42.06	40.81
Average	44.98	44.19	42.28	40.91	40.29	39.86	38.48

4.2 Image Quality Comparison of Related Methods

This section compares the embedding capacity based on each method and observes the value of PSNR after hiding the embedded secret information. Figures 6 (a) (f) present the visualized data graphs of the relative changes of EC and PSNR when the six test images were gradually embedded with data until the maximum embedding capacity attained that each image can carry.

4.2.1 HoVo_DE Embedding Strategy Applied to the DE Method

Figures 6 (a)-(f) show that in the HoVo_DE_3×3, HoVo_DE_4×4, HoVo_DE_5×5, or HoVo_DE_6×6 methods, the maximum embedding capacity of each proposed method is much higher than that of BSE_1×4 or BSE_2×2. Also, the maximum embedding capacity of the HoVo_DE_6×6 method can achieve 1.654 bpp on average. Although the image quality decreases with an increase in embedding capacity, the PSNR of the HoVo_DE embedding strategy cannot be far from the methods of BSE_1×4 or BSE_2×2. Consider the Airplane image in Figures 6(a) as an example when the embedding capacity is 1 bpp, the PSNR of the BSE_2×2 method is 30.58 dB, and the PSNR of the HoVo_DE_6×6 method is 28.9 dB, where the image quality difference between the two methods under the same EC is less than 2 dB. However, our proposed HoVo_DE_6×6 method can achieve a maximum embedding capacity of 1.654 bpp.

4.2.2 HoVo_DE Embedding Strategy Applied to the IRDE Method

Figures 7(a)-(f) show that the proposed method proposed can significantly increase the EC. The maximum EC of the HoVo_IRDE_6×6 methods can reach 1.6 bpp, and the image quality can still maintain the PSNR above 40 dB, such as in Airplane, Lena, and Peppers. This means that our proposed block segmentation can suppress the effect of the difference expansion cascading to a certain extent. Also, the overlapping mechanism can offset the pixel differential value of the upper layer expansion. Consider Figure 7(a) as an example when the test image is an airplane and the embedding capacity is 1 bpp, the PSNR of the BSE_2×2 method is 42.41 dB. The PSNR values of our method slightly outperform those of the BSE_2×2 methods. This shows that the HoVo_DE embedding strategy has better image quality and larger embedding capacity than the BSE method at the same level of EC.

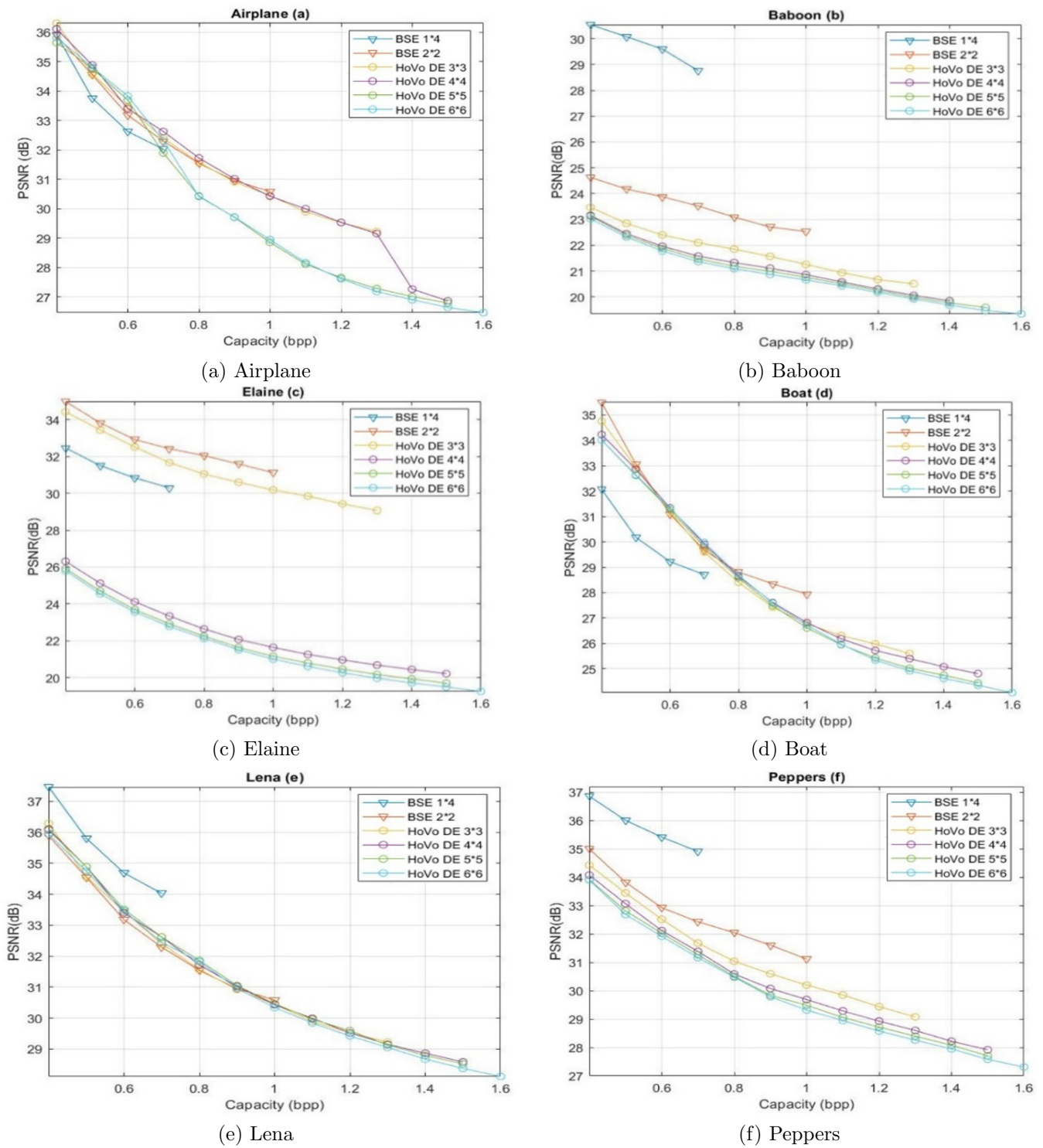


Figure 6: The performance of BES method and HoVo_DE method in image quality under different embedding capacity

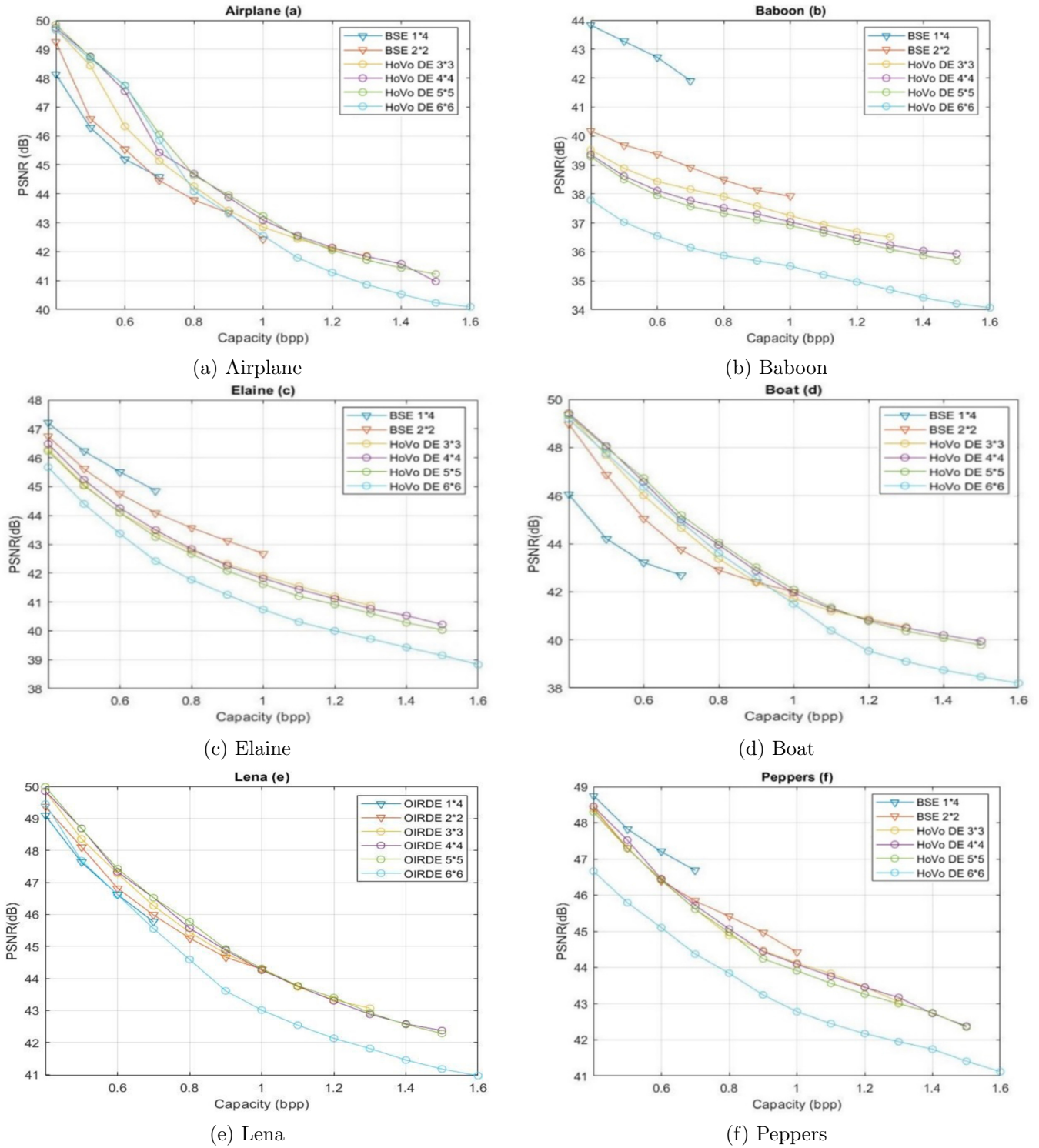


Figure 7: The performance of BES method and HoVo_IRD Emethod in image quality under different embedding capacity

4.3 Comparison of Image Quality Effects of HoVo_DE Embedding Strategy Implemented in Multi-layer Embedding

This study applies the HoVo_DE embedding strategy to multi-layer embedding. The stego-image generated by the original image using the HoVo_DE strategy through one layer of embedding becomes the input of the second layer of data hiding. This embedding method is called two-layer embedding. The following presents the image quality and embedding capacity obtained by the two-layer embedding based on the proposed HoVo_DE embedding strategy under different block-division modes.

Table 5 shows that the average embedding capacity of HoVo_DE.3×3 in a single layer embedding manner is 344951 bits, and the average embedding capacity of HoVo_DE.3×3 in a two-layer embedding manner can reach 643779 bits, which is an increase of 298828 bits compared with a single layer embedding. Taking the HoVo_DE.6×6 as an example, the average embedding capacity of the HoVo_DE.6×6 method is 430226 bits in a single layer embedding and 803300 bits in a two-layer embedding, which is an increase of 373074 bits compared with a single layer. However, the image quality also decreases with a larger EC. As shown in Table 5, whether it is the HoVo_DE.3×3, HoVo_DE.4×4, HoVo_DE.5×5, or HoVo_DE.6×6 methods, although the block sizes are different, their average embedding capacity in the two layers is 200% more than that in only one-layer embedding.

Figure 8 shows the average performance of six test images when the HoVo_DE embedding strategy is applied to two layers based on the DE method and as HoVo_DE.3×3(2L) when using the HoVo_DE.3×3 method to hide data with two-layer embedding. Similarly, when using HoVo_DE.4×4, HoVo_DE.5×5, and HoVo_DE.6×6 to hide data with two-layer embedding, they can be represented as HoVo_DE.4×4(2L), HoVo_DE.5×5(2L), and HoVo_DE.6×6(2L), respectively. In Figure 8, although the image quality suffers, the embedding capacity of the two layers can be improved significantly. Taking the HoVo_DE.6×6 method as an example, the average embedding capacity of a single layer HoVo_DE.6×6 is 1.6 bpp, and its PSNR value is about 25 dB. The average maximum embedding capacity of HoVo_DE.6×6(2L) can reach 3 bpp.

Table 5: Comparison of EC of single-layer and two-layer embedding based on HoVo DE method

EC	HoVo DE 3×3	HoVo DE 3×3	HoVo DE 4×4	HoVo DE 4×4	HoVo DE 5×5	HoVo DE 5×5	HoVo DE 6×6	HoVo DE 6×6
	1 Layer	2 Layer	1 Layer	2 Layer	1 Layer	2 Layer	1 Layer	2 Layer
Airplane	346252	674841	392637	769230	415566	812326	432859	843257
Baboon	341373	599241	386262	695117	408236	731742	424544	751410
Elaine	345374	593427	390707	683417	412548	716995	429477	734892
Boat	345287	649330	391277	741300	413895	782065	430811	808887
Lena	346604	677374	393034	772859	415944	815799	433263	847457
Peppers	344814	668460	390648	761519	413361	803383	430403	833896
Average	344951	643779	390761	737240	413258	777052	430226	803300

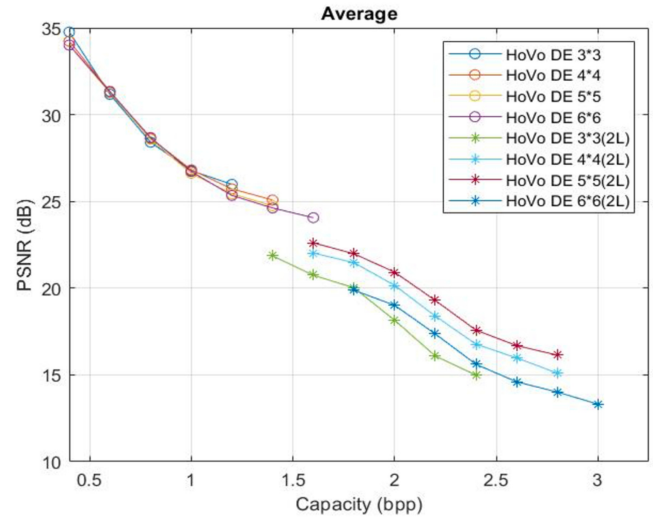


Figure 8: The average image quality vs embedding capacity of the first and second layer embedding based on the DE method, the HoVo_DE embedding strategy is applied to different block division modes

Table 6 shows that the average embedding capacity of HoVo_IRDE.3×3 in a single layer is 346786 bits, while the average embedding capacity of HoVo_IRDE.3×3 using two layers can reach 693332 bits, which is an increase of 346546 bits compared to a single layer embedding; the average embedding capacity of HoVo_IRDE.4×4 in a single layer is 393197 bits, while the average embedding capacity of HoVo_IRDE.4×4 using two layers can reach 786602 bits, which is an increase of 393405 bits compared to a single layer embedding; the average embedding capacity of HoVo_IRDE.5×5 in a single layer is 416154 bits, while the average embedding capacity of HoVo_IRDE.5×5 using two layers can reach 832570 bits, which is an increase of 416416 bits compared to a single layer embedding; the average embedding capacity of HoVo_IRDE.6×6 in a single layer is 433496 bits, while the average embedding capacity of HoVo_IRDE.6×6 using two layers can reach 867025 bits, which is an increase of 433529 bits compared to a single layer embedding. The embedding capacity can be improved significantly compared to the single layer and the PSNR values using two-layer embedding has can attain a level above 30 dB as shown in Figure 9.

Table 6: Comparison of EC of single-layer and two-layer embedding based on HoVo_IRDE method

EC	HoVo DE 3×3	HoVo DE 3×3	HoVo DE 4×4	HoVo DE 4×4	HoVo DE 5×5	HoVo DE 5×5	HoVo DE 6×6	HoVo DE 6×6
	1 Layer	2 Layer	1 Layer	2 Layer	1 Layer	2 Layer	1 Layer	2 Layer
Airplane	346804	693605	393217	786434	416154	832180	433473	866974
Baboon	346801	693355	393215	786799	416139	833031	433516	867113
Elaine	346805	693537	393117	786320	416191	832352	433506	866817
Boat	346764	693433	393186	786685	416182	832705	433455	867147
Lena	346801	692906	393207	786678	416161	832458	433501	867288
Peppers	346738	693159	393127	786695	416098	832691	433524	866813
Average	346786	693332	393197	786602	416154	832570	433496	867025

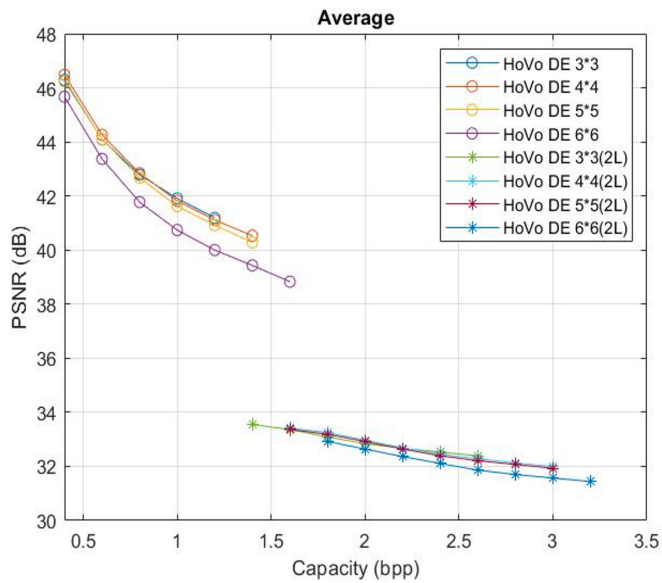


Figure 9: The average image quality vs embedding capacity of the first and second layer embedding based on the IRDE method, the HoVo_DE embedding strategy is applied to different block division modes

5 Conclusions

The traditional DE embedding method is usually in sequential order when it is used to embed secret data; for example, the pixels are embedded individually from left to right. However, with each embedding, the difference continues to expand, causing the difference expansion cascading problem which results in bad embedding capacity. Therefore, when performing the embedding operation, the proposed HoVo_DE embedding strategy abandons the traditional left to right order to perform pixel embedding individually and uses a block as a unit which is then subdivided into groups. Then, the information from the groups at both ends of the block is embedded into the center position group in an overlapping manner. Simultaneously, this strategy checks whether there is an overflow of the camouflaged pixel value each time the secret data are embedded, which can maximize the embedding capacity of secret data and offset the subsequent embedding to a certain extent.

We implemented the HoVo_DE embedding strategy in 3×3 , 4×4 , 5×5 , and 6×6 block division modes. The experimental results indicated that the size of the different blocks increases the embedding capacity and maintains a similar level of image quality. The study also found that the additional embedding capacity decreases each time with a linear curve when larger block size is adopted. This means that the effect of the exchange of the embedding capacity with a larger block-division mode becomes increasingly limited. We also found that when the block size is greater than 5×5 , the embedding capacity does not continue to increase significantly, especially when ob-

erving the 5×5 and 6×6 blocks. Also, the image quality slows down with the linear curve reduction. Also, experiments have shown that using multi-layer embedding to obtain additional embedding capacity will also face the problem of a sharp drop in image quality. To sum up, the HoVo_DE embedding strategy indeed addresses the difference expansion cascading problem, enhances the embedding capacity, and maintains good image quality.

Acknowledgments

This research was partially supported by the Ministry of Science and Technology, Taiwan, Republic of China under the Grant [MOST 111-2221-E-324-019-MY2]. The authors also gratefully acknowledge the helpful comments and suggestions of the reviewers, which have improved the quality.

References

- [1] A. M. Alattar, "Reversible watermark using difference expansion of quads," in *2004 IEEE International Conference on Acoustics, Speech, and Signal Processing*, pp. iii-377-80, Montreal, QC, Canada, May 2004.
- [2] A. M. Alattar, "Reversible watermark using the difference expansion of a generalized integer transform," *IEEE Transactions on Image Processing*, vol. 13, pp. 1147-1156, 8 2004.
- [3] C. K. Chan and L. M. Cheng, "Hiding data in images by simple lsb substitution," *Pattern Recognition*, vol. 37, pp. 469-474, 3 2004.
- [4] M. Hussain, A. W. A. Wahab, Y. I. BinIdris, A. T. S. Ho, and K. H. Jung, "Image steganography in spatial domain: A survey," *Signal Processing: Image Communication*, vol. 65, pp. 46-66, 7 2018.
- [5] N. F. Johnson and S. Jajodia, "Exploring steganography: Seeing the unseen," *Computer*, vol. 31, pp. 26-34, 2 1998.
- [6] I. J. Kadhim, P. Premaratne, P. J. Vial, and B. Hal-loran, "Comprehensive survey of image steganography: Techniques, evaluations, and trends in future research," *Neurocomputing*, vol. 335, pp. 299-326, 3 2019.
- [7] H. J. Kim, V. Sachnev, Y. Q. Shi, J. Nam, and H. Choo, "A novel difference expansion transform for reversible data embedding," *IEEE Transactions on Information Forensics and Security*, vol. 3, pp. 456-465, 9 2008.
- [8] C. F. Lee, H. L. Chen, and H. K. Tso, "Embedding capacity raising in reversible data hiding based on prediction of difference expansion," *The Journal of Systems and Software*, vol. 83, pp. 1864-1872, 10 2010.
- [9] C. F. Lee, J. J. Shen, Y. J. Wu, and S. Agrawal, "Reversible data hiding scheme based on difference

- expansion using shiftable block strategy for enhancing image fidelity,” in ,” *IEEE 10th International Conference on Awareness Science and Technology (iCAST)*, pp. 1–6, Morioka, Japan, October 2019.
- [10] C. F. Lee, C. Y. Weng, C. H. Wang, G. Chakraborty, K. Sakurai, and K. Y. Tsai, “Research on multimedia application on information hiding forensics and cybersecurity,” *International Journal of Network Security (IJNS)*, vol. 23, pp. 1093–1107, 11 2021.
- [11] X. Li, J. Li, B. Li, and B. Yang, “High-fidelity reversible data hiding scheme based on pixel-value-ordering and prediction-error expansion,” *Signal Processing*, vol. 93, pp. 198–205, 1 2013.
- [12] C. L. Liu, D. C. Lou, and C. C. Lee, “Reversible data embedding using reduced difference expansion,” in *Third International Conference on Intelligent Information Hiding and Multimedia Signal Processing (IIH-MSP 2007)*, pp. 433–436, Kaohsiung, Taiwan, November 2007.
- [13] Z. Ni, Y. Q. Shi, N. Ansari, and W. Su, “Reversible data hiding,” in *Proceedings of the 2003 International Symposium on Circuits and Systems (ISCAS)*, vol. 2, pp. 912–915, Bangkok, Thailand, May 2003.
- [14] D. M. Thodi and J. J. Rodriguez, “Reversible watermarking by prediction-error expansion,” *6th IEEE Southwest Symposium on Image Analysis and Interpretation*, pp. 21–25, 3 2004.
- [15] J. Tian, “Image steganography in spatial domain: A survey,” *IEEE Transactions on Circuits and Systems for Video Technology*, vol. 13, pp. 890–896, 8 2003.
- [16] D. C. Wu and W. H. Tsai, “A steganographic method for images by pixel-value differencing,” *Pattern Recognition Letters*, vol. 24, pp. 1613–1626, 2003.
- [17] H. Yi, S. Wei, and J. Hou, “Improved reduced difference expansion based reversible data hiding scheme for digital images,” in *2009 9th International Conference on Electronic Measurement & Instruments*, pp. 4–315–4–318, Beijing, China, August 2009.

Biography

Chin-Feng Lee received her Ph.D. in Computer Science and Information Engineering from National Chung Cheng University, Taiwan in 1998. She is currently a professor of Information Management at Chaoyang University of Technology, Taiwan. Her research interests include steganography, image processing, information retrieval and data mining.

Jau-Ji Shen received his Ph.D. in Computer Science and Information Engineering from National Taiwan University, Taiwan in 1988. He is currently a professor of Information Management at Chung Hsing University, Taiwan. His research interests include image techniques, data techniques and software engineering.

Chin-Yung Wu received his Master degree in Information Management at Chung Hsing University, Taiwan. His research interests include image techniques, and data hiding.